

Study of the resistive switching and electrode degradation in Al/TiO₂/FTO thin films upon thermal treatment in reducing atmosphere

G. A. Illarionov¹, D. S. Kolchanov¹, V. V. Chrishtop¹, I. A. Kasatkin², A. V. Vinogradov¹, M. I. Morozov¹

¹ITMO University, Kronverkskiy prosp., 49, St. Petersburg, 197101, Russia

²Saint Petersburg State University, Universitetskaya nab. 7-9, St. Petersburg, 199034, Russia

morozov@scamt-itmo.ru

PACS 81.40.Rs, 73.50.-h

DOI 10.17586/2220-8054-2021-12-6-783-791

Application of sol-gel derived titania nanoparticles in memristive thin film devices has been a subject of several studies. The reported data on the functional properties and stability of such devices scatter considerably. Meanwhile, the role of post-fabrication treatment, such as annealing in reducing atmosphere, is still poorly investigated for this class of devices. In this study, the effects of thermal annealing in a reducing atmosphere on the resistive switching behavior and the morphological changes of the top electrode during the electroforming process have been systematically addressed for the samples of Al/TiO₂/FTO thin film memristors prepared using sol-gel derived titania. Manifestations of several phenomena affecting the functional stability of these thin films, such as electrode delamination and collapse due to formation of gas bubbles, appearance of electrochemical patterns at the electrode surface, and morphological changes induced by the electroforming process have been systematically established in relation with the various conditions of thermal treatment in a reducing atmosphere.

Keywords: TiO₂, memristors, electrode degradation.

Received: 25 November 2021

1. Introduction

The field of memristive electronics is one of the promising areas of rapidly developing technologies covering novel types of memory devices and bioinspired computers [1–4]. Memristor is a passive two-terminal element of electric circuit, whose resistance dynamically depends on of the electric current amplitude [5]. This key feature has been proposed for application in the information storage [6, 7] or emulation of similar electrical processes in biological synapses [8–10]. The memristive effect occurs in many organic and inorganic nanomaterials including simple oxides of transition metals.

Titanium dioxide has been one of the first and most widely used materials in resistive switching applications. Since the first conceptual implementation of memristive effect in TiO₂ thin films [3], this material has been extensively studied regarding both the underlying mechanism of the resistive switching, various applications, as well as technological approaches towards design and fabrication of final devices [11–13]. The frontier research and application of TiO₂ memristors concern random-access memory [13–16], neuromorphic computing [3, 17–19], biohybrid interfaces [20–23], and sensors [24–27]. The key advantages of TiO₂ thin film memristors include a relatively high resistive switching ratio R_{OFF}/R_{ON} (typically, much above 10²), low threshold voltage (typically, 1-3 volts), and technological versatility of the fabrication methods [12, 13]. Meanwhile, TiO₂ memristors are rather inferior to other transition oxide counterparts with respect to the functional endurance that in most reported cases has not exceeded a few hundred cycles [13], though in some episodic studies some higher values above 10⁴-10⁶ have been reported [28–31]. However, this range is still far below compared to the TaO_x counterparts with endurance typically exceeding 10⁹–10¹⁰ cycles [32, 33]. Another obvious disadvantage of TiO₂ based memristor is apparently low reproducibility that manifested itself in an extremely large scattering of the functional properties reported for the films fabricated by similar to each other technological methods and synthesis routes [12, 13].

Recently, several studies have addressed the solution chemistry approaches to synthesize TiO₂ nanoparticles along with appropriate deposition methods to fabricate thin film memristors, including spin-coating [34, 35], dip coating [36–38], drop casting [39], or inkjet printing [40, 41]. In contrast to memristive devices produced by the physical deposition techniques, an extremely high scattering of the key memristive properties such as the resistive switching ratio, endurance and retention time have been reported for the devices fabricated using TiO₂ nanoparticles obtained by the solution chemistry routes [12]. In these studies, different electrode materials and post-treatment annealing regimes have been used, while the effect of thermal annealing at a reduced oxygen partial pressure on the resistive and resistive switching properties of TiO₂ thin film has not been systematically addressed yet. Another critical issue rarely addressed for the memristive devices fabricated using TiO₂ nanoparticles is the degradation of the top electrode as the result of electrochemical interaction with the TiO₂ adjacent layer under applied external voltage. This includes

formation and collapse of oxygen bubbles under the metal layer [42–44] and damages produced by the morphological changes resulting from the electroforming process [45–47].

In this study, we investigate the effect of thermal annealing at various temperatures in Ar atmosphere on the resistive switching manifestation of an Al/TiO₂/FTO thin film memristor fabricated using sol-gel derived TiO₂ nanoparticles deposited onto FTO glass by spin-coating and covered by top Al electrodes using thermal evaporation. Additionally, we address the effect of top electrode degradation as the result of electrochemical interactions occurring during the switching upon various stages of thermal annealing in oxygen reducing atmosphere.

2. Materials and Methods

2.1. Chemicals

Titanium(IV) isopropoxide (97%, Sigma-Aldrich), nitric acid (65%, Sigma-Aldrich), deionized water ($<5 \mu\text{S}\cdot\text{cm}^{-1}$), isopropanol ($\geq 99.9\%$, Vekton), methanol ($\geq 99.8\%$, Fisher Scientific).

2.2. TiO₂ synthesis

TiO₂ sol was synthesized via sol-gel procedure. Two solutions were prepared. For the first solution 16 mL of titanium isopropoxide and 12 mL of 2-propanol were mixed. For the second solution 0.7 mL of nitric acid was added to 100 mL of water and heated up to 70 °C. After that, the first solution was slowly added to the second one under constant stirring. The resulting mixture was maintained for 1 h at 80 °C then hermetically covered by a film and kept for 5 days under stirring at room temperature.

2.3. TiO₂ ink preparation

The synthesized sol was dried in a vacuum evaporator to form TiO₂ xerogel. Then, TiO₂ ink was obtained by mixing aqueous solution of TiO₂ xerogel (20%) with methanol in a ratio of 1:3.

2.4. Thin film fabrication

Fluorine-doped tin oxide (FTO) glass substrates (25×25×2 mm, $<10 \Omega\cdot\text{cm}^{-2}$, FTO thickness 950 nm) were treated in an ultrasonic bath for 5 minutes sequentially in 5 solutions: NaOCl, NaHCO₃, deionized water, isopropyl alcohol, and acetone, then dried with N₂ flow. The surface hydrophilization was performed in air plasma for 10 minutes using a Femto Low Pressure Plasma System (Diener Electronic GmbH, Germany). After that, one layer of prepared TiO₂ ink was spin coated onto the precleaned and hydrophilized FTO using a spin coater APT Spin – 150i NPP (SPS Europe, France). The coating was performed as one-step procedure with the following parameters: spin speed 2500 rpm, acceleration 350 rpm, time 45 sec. The top Al electrodes were deposited by thermal evaporation in a vacuum chamber.

2.5. Top electrode deposition

Aluminum layer with a thickness of 50 nm was deposited onto TiO₂ layer by thermal evaporation in a vacuum chamber using a mask with circular holes. The surface area of each Al electrode was set to be 5.85 mm². The resulting array of the sandwiched TiO₂ layer memristors with the common bottom FTO electrode is illustrated in Fig. 1a. The thickness of the functional TiO₂ layer was evaluated by atomic force microscopy (AFM) using a Solver Next microscope (NT-MDT, Russia). As illustrated in Fig. 1b, the thickness of the TiO₂ layer was estimated to be ca. 60 nm.

2.6. Thermal treatment

After each electrical and microscopical examination, the sample was annealed in Ar for at least 12 h at 250, 350 and 500 °C using a tube furnace LOIP LF-50/500-1200. The ramp rate was set to 3 °C/min.

2.7. Material characterization

Images of the electrode surface were taken using a LOMO Biolam M-1 microscope equipped with a Micro-metrics 519CU CMOS 5.0 camera. Scanning electron microscopy (SEM) images were obtained using an electron microscope Tescan Vega 3. Energy dispersive X-ray spectroscopy (EDX) mapping was performed using an X-act Silicon Drift Detector from Oxford Instruments. Phase composition at the film surface was analyzed by the X-ray diffraction (XRD) using a Bruker D8 Discover X-ray diffractometer with filtered parallel beam CuK_α radiation in grazing incidence regime. The current – voltage dependencies were measured using a SubFemtoamp SourceMeter Keithley 6430 controlled by KickStart Instrument Control Software Version 2.0.6 (Tektronix). Voltage was applied with a wire tip connected to the Al top electrode, while another wire was connected to the bottom FTO electrode.

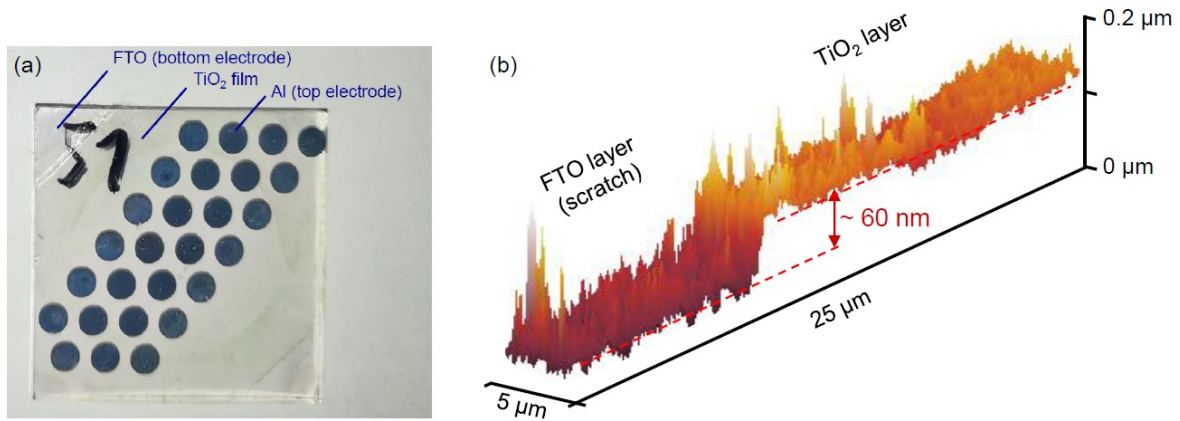


FIG. 1. (a) Experimental sample of Al/TiO₂/FTO memristors; (b) AFM characterization of TiO₂ layer thickness

3. Results and discussion

In this section we present and discuss the results of electrical characterization of Al/TiO₂/FTO thin film memristors along with morphological changes of the top electrode surface before and after several stages of annealing in Ar at 250, 350, and 500 °C, correspondingly.

3.1. Unannealed film

The positive and negative voltage-current curves obtained for an unannealed Al/TiO₂/FTO thin film are shown in Fig. 2. The insets depict images of the top electrode surfaces taken after each 20 negative and positive cycles. At negative polarity, no visible degradation was observed for the top Al electrode, while no notable resistive switching has been observed. At positive polarity, the current amplitude has been gradually descending during the cycling, which corresponds to the formation of gas bubbles resulting in partial delamination of the aluminum layer thus reducing the contact area. Similar formation of the gas bubbles was documented in several studies including the cases of SrTiO₃ single crystal with Au electrode [42] and Pt-TiO₂-Pt thin films fabricated with the sandwiched [43] and planar [44] configurations. The mechanism of the gas bubble formation under the anode was studied in detail [43] and rationalized by the drift of O₂⁻ anions towards the positively biased top electrode followed by the discharging with the subsequent formation of O₂ gas between TiO₂ and the top electrode. Consequently, the drift of oxygen vacancies occurs in the opposite direction [6]. Despite this evidence of the ionic drift manifestation, no filamentary resistive switching was observed in the unannealed thin film.

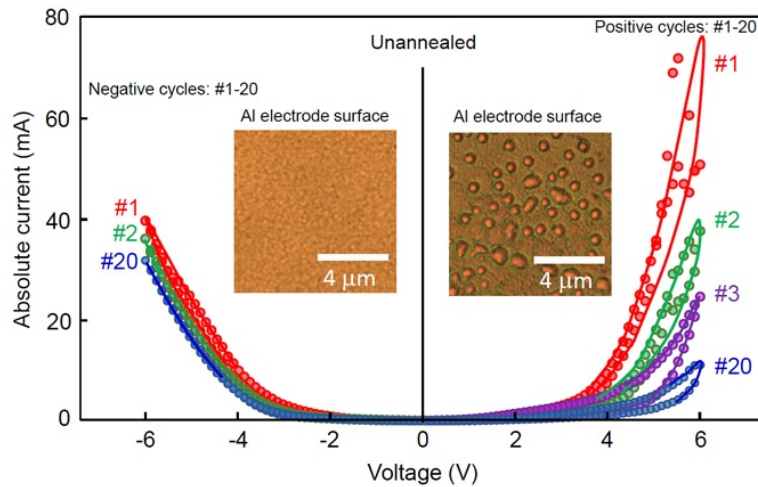


FIG. 2. Positive and negative I-V curves for Al/TiO₂/FTO thin film and the effect of positive and negative cycles on the top Al electrode

3.2. Characterization upon annealing at 250 °C in Ar

Fig. 3a depicts the positive and negative voltage - current curves obtained for a sample of Al/TiO₂/FTO thin film annealed in Ar at 250 °C. An appreciably high resistive switching ratio R_{OFF}/R_{ON} above 10^4 was obtained in the sub-switching characterization regime, as illustrated in Fig. 3b.

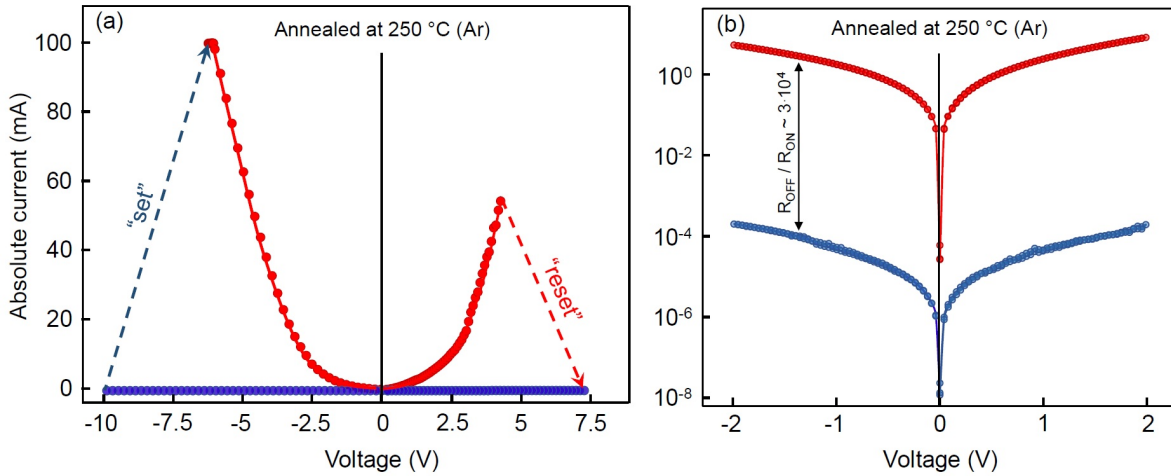


FIG. 3. I-V characterization of Al/TiO₂/FTO thin film annealed in Ar at 250 °C: (a) negative and positive switching curves; (b) sub-switching curves in the “OFF” and “ON” states

The activation of the resistive switching to the “ON” state has been investigated in detail by application of elongated voltage pulses with stepwise changing amplitude, as illustrated in Fig. 4. The primary switching event was observed at voltage pulse amplitude of -6 V (Fig. 4a) upon nearly a minute since the pulse had been applied (Fig. 4b). This observation is in line with a model of the resistive switching mechanism based on filament formation [6, 48, 49]. In contrast, the reverse processes observed upon changing the polarity have demonstrated rather slow dynamics of current relaxation, as shown by the U-I curves 11–13 in Fig. 4b.

Upon several bipolar cycles, the resistive switching in Al/TiO₂/FTO thin film annealed in Ar at 250 °C became unstable. As exemplified in Fig. 5, several set-reset switching fails have been observed at relatively low voltage.

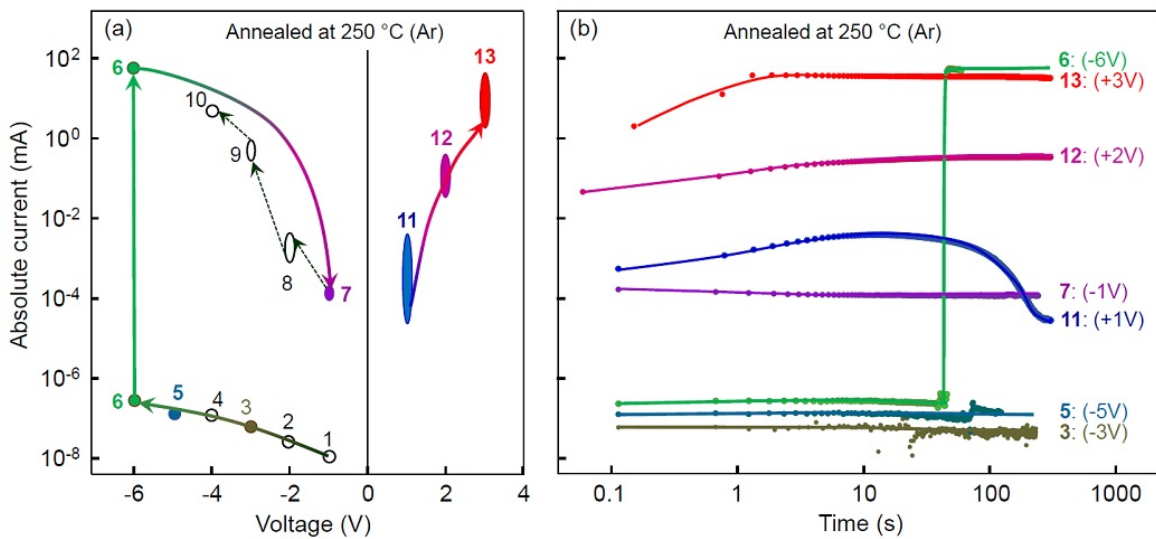


FIG. 4. Electrical switching cycle in Al/TiO₂/FTO thin film annealed in Ar at 250 °C: (a) the resistive switching process measured with elongated voltage pulses; (b) the corresponding current curves as a function of time for the stepwise varying voltage measured for the selected points shown in (a)

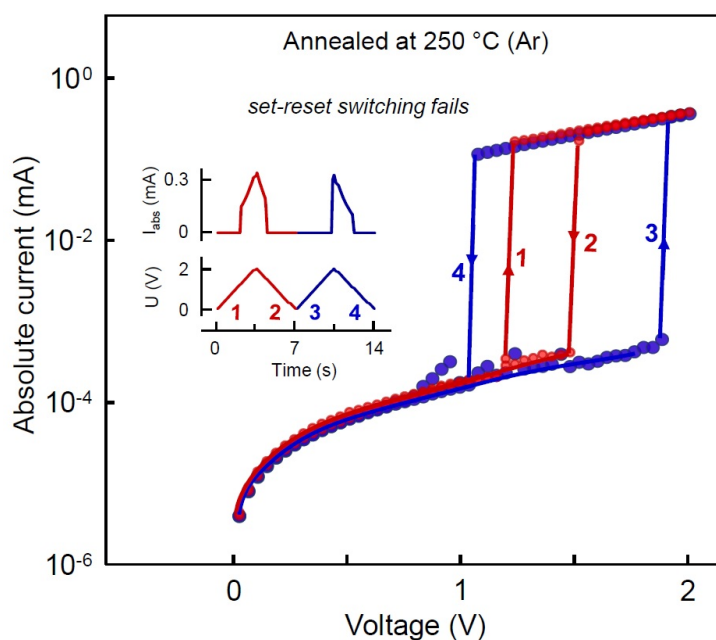


FIG. 5. Instability of resistive switching in Al/TiO₂/FTO thin film annealed in Ar at 250 °C. The inset illustrates the corresponding applied voltage pulses and the current response as functions of time

Inferior functional endurance and retention of the resistive switching memory devices based on TiO₂ have been reported in several studies, especially those addressing solution chemistry approaches to the synthesis of the primary nanoparticles [12, 13, 50]. The reasons for this phenomenon are still poorly understood. However, one of the known factors affecting the stability of resistive switching is degradation and morphological changes in the electrodes induced by electroforming and switching [51, 52]. The state of the electrode surface in a sample of Al/TiO₂/FTO thin film annealed in Ar at 250 °C and subjected to several resistive switching cycles have been observed using optical and scanning electron microscopy with EDX analysis. The results are shown in Fig. 6. The optical microscopy (Fig. 6a) revealed traces of electrochemical patterns that are typical for the aluminum electropolishing process [53, 54]. This suggests that the thermal treatment at 250 °C was not sufficient for complete removal of the acidic substances used for the synthesis of TiO₂ nanoparticles. Furthermore, some local delaminated spots of the Al electrode with circular profile evidenced on the SEM microphotograph (Fig. 6b) and EDX aluminum map (Fig. 6c) indicate the formation of gas bubbles with their consequent outbreak through the Al electrode. Thus, the examined thermal treatment was also not sufficient to achieve the concentration of oxygen vacancies in the TiO₂ layer at a level required for the resistive switching. For these reasons, further examination was conducted upon thermal treatment in Ar at 350 °C.

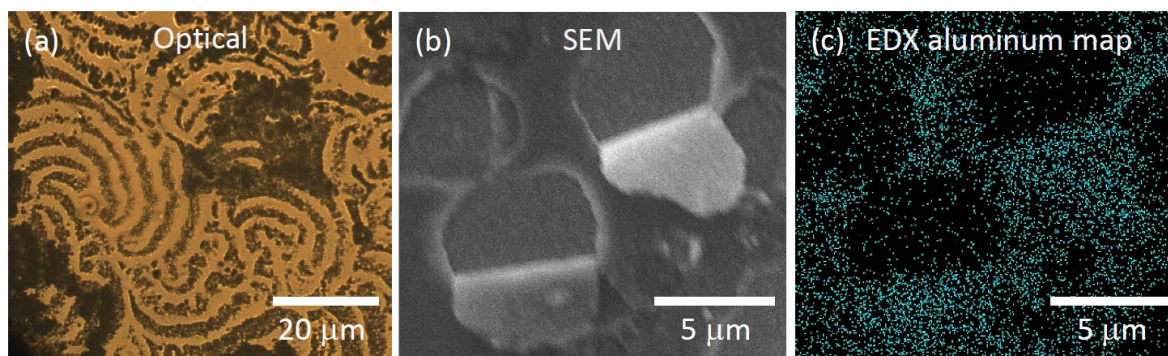


FIG. 6. (a) Optical microscopy, (b) SEM, and (c) EDX (Al mapping) images taken from the top aluminum electrode of the Al/TiO₂/FTO thin film sample annealed in Ar at 250 °C and subjected to several bipolar resistive switching cycles

3.3. Characterization upon annealing at 350 °C in Ar

Fig. 7a shows the first three bipolar switching cycles measured in response to the applied voltage pulses with stepwise increasing amplitude for the sample of Al/TiO₂/FTO thin film annealed in Ar at 350 °C. The observed resistive switching ratio R_{OFF}/R_{ON} in this case remained above 10^4 , as exemplified in Fig. 7b. However, the instability of the set-reset resistive switching voltage persisted (Fig. 7b). A magnified image of the top electrode surface (Fig. 8) indicates the presence of minor traces of electrochemical pattern, which is in contrast to the case of the sample annealed in Ar at 250 °C. Furthermore, no traces of collapsed gas bubbles were observed. However, the morphological changes induced by the electroforming process persisted in this sample as well. Similar observations were reported in literature for other configurations of TiO₂ memristor, including the cases with Pt electrodes [51,52]. At the next stage, an examination of an Al/TiO₂/FTO thin film was carried out upon thermal annealing in Ar at 500 °C.

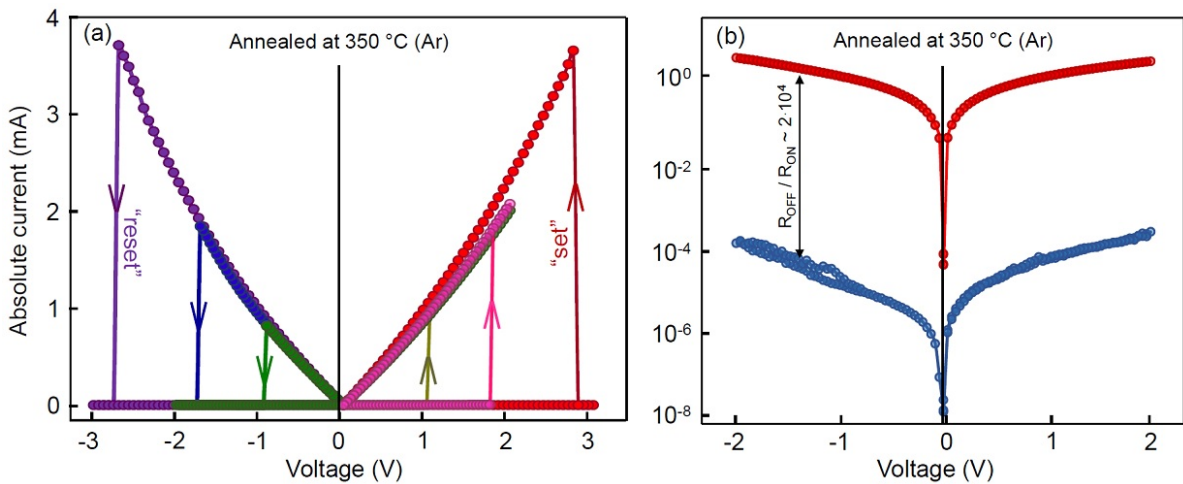


FIG. 7. I-V characterization of Al/TiO₂/FTO memristive film annealed in Ar at 350 °C: (a) The first three bipolar switching cycles measured at stepwise increasing amplitude of the applied voltage pulses; (b) sub-switching curves in the "OFF" and "ON" states

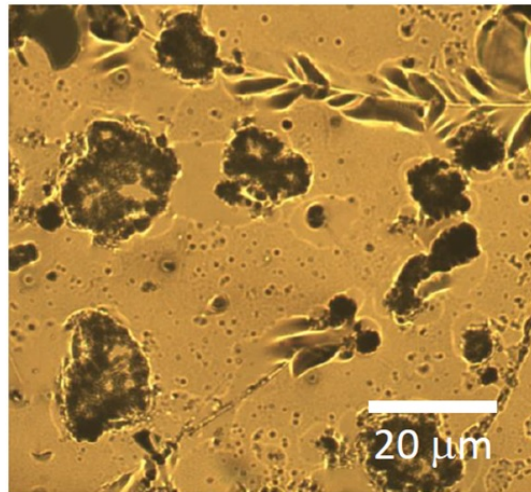


FIG. 8. Optical microphotograph of the top aluminum electrode surface in the Al/TiO₂/FTO thin film sample annealed in Ar at 350 °C

3.4. Characterization upon annealing at 500 °C in Ar

Samples of Al/TiO₂/FTO thin film annealed in Ar at 500 °C have been characterized at various voltage regimes. They showed no reversible switching of the electrical resistance. As exemplified in Fig. 9a, a slow non-filamentary current increase was observed at a rectangular voltage pulses with 4V amplitude, however this process was unstable

and followed by a rapid decay (curve # 4). Further increase in the applied voltage have resulted in a similar behavior: a gradual increase in the current response followed by a rapid drop, as illustrated in Fig. 9b.

A microphotograph of the top electrode surface is shown in Fig. 10a. It appears to be rough and porous. An XRD analysis performed at the grazing incidence geometry for the sample of Al/TiO₂/FTO thin film annealed in Ar at 500 °C has revealed the formation of a secondary phase, as marked by asterisks in Fig. 10b. This suggests that the applied annealing conditions likely induced an irreversible chemical interaction resulting in the formation of a secondary phase, which seemingly suppresses the resistive switching of the thin film.

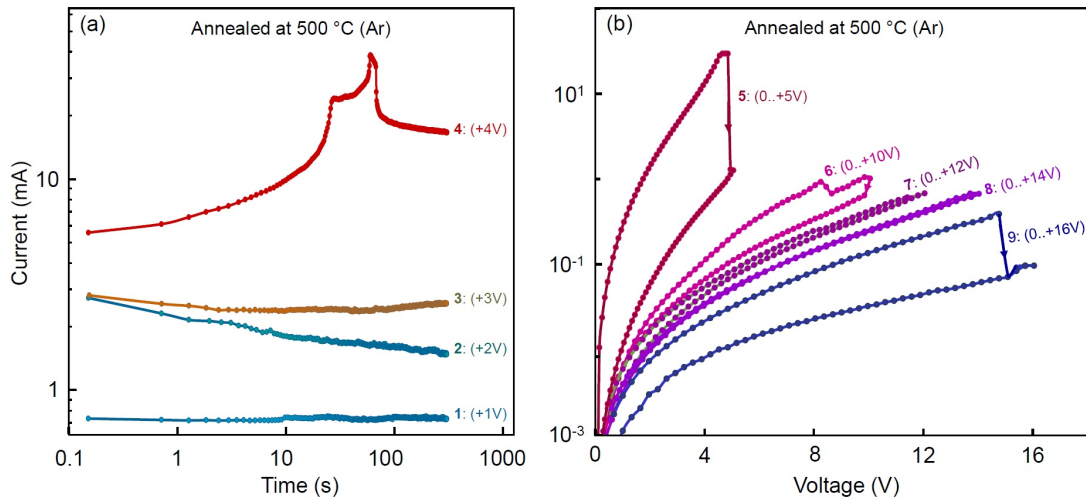


FIG. 9. I-V characterization of Al/TiO₂/FTO thin film annealed in Ar at 500 °C. The first nine unipolar cycles with stepwise increasing amplitude of the applied voltage: (a) the first four cycles as a function of time; (b) the next five cycles as I-V hystereses

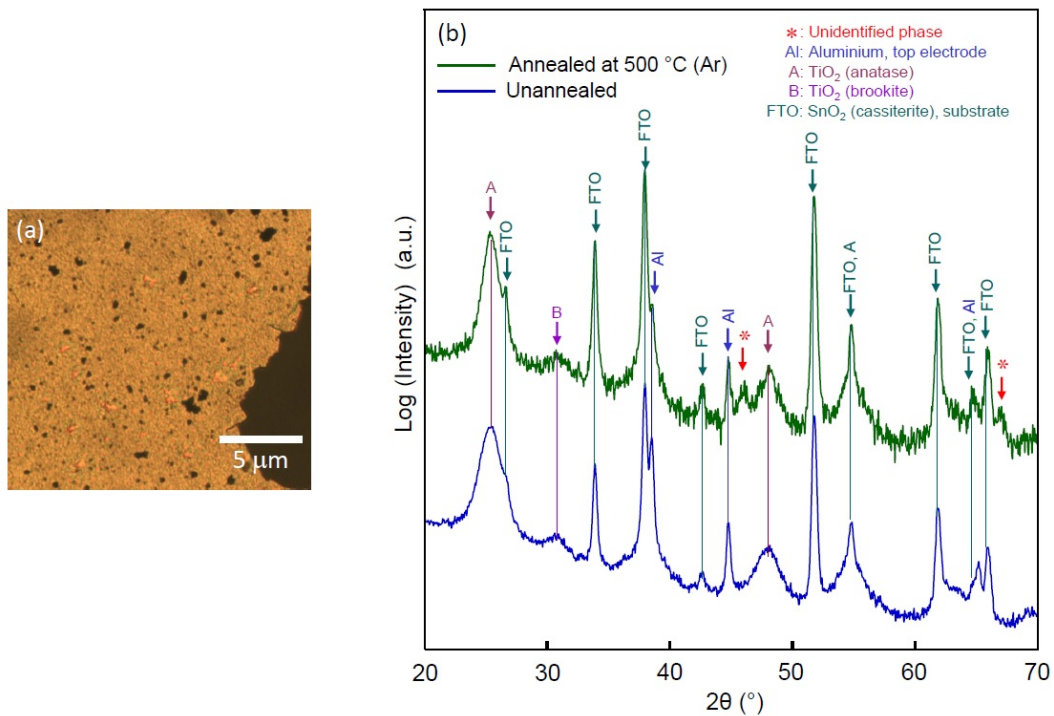


FIG. 10. (a) Optical microphotograph of the top aluminum electrode surface in the Al/TiO₂/FTO thin film sample annealed in Ar at 500 °C and (b) XRD spectra taken in the grazing incidence geometry from the same surface and the surface of an unannealed sample

4. Conclusion

In this study, the effect of thermal annealing in a reducing atmosphere on the resistive switching behavior and the morphological changes of the top electrode during the electroforming process have been systematically addressed for samples of Al/TiO₂/FTO thin film memristors prepared using sol-gel derived titania. Manifestations of several phenomena affecting the functional stability of these thin films, such as electrode delamination and collapse due to formation of gas bubbles, appearance of electrochemical patterns on the electrode surface, and morphological changes induced by the electroforming process have been established in relation with the various conditions of thermal treatment in a reducing atmosphere. The temperature limit for the post-fabrication treatment has also been established. Thermal treatment at 500 °C or above was shown to induce irreversible phase transformation due to chemical interaction, despite the treatment being performed in an inert atmosphere.

Acknowledgement

The research has been carried out with financial support from the Russian Science Foundation (Grant No. 19-19-00433).

References

- [1] Yang J.J., Strukov D.B., Stewart D.R. Memristive devices for computing. *Nat. Nanotechnol.*, 2012, **8**, P. 13–24.
- [2] Zidan M.A. The future of electronics based on memristive systems. *Nat. Electron.*, 2018, **1**, P. 22–29.
- [3] Zhang Y., Wang Z., Zhu J., Yang Y., Rao M., Song W., Zhuo Y., Zhang X., Cui M., Shen L., Huang R., Yang J.J. Brain-inspired computing with memristors: challenges in devices, circuits, and systems. *Appl. Phys. Rev.*, 2020, **7**, P. 011308.
- [4] Velichko A., Belyaev M., Boriskov P. A Model of an Oscillatory Neural Network with Multilevel Neurons for Pattern Recognition and Computing. *Electronics*, 2019, **8**(1), P. 75.
- [5] Strukov D.B., Snider G.S., Stewart D.R., Williams R.S. The Missing Memristor Found. *Nature*, 2008, **453**(7191), P. 80–83.
- [6] Waser R., Dittmann R., Staikov G., Szot K. Redox-Based Resistive Switching Memories – Nanoionic Mechanisms, Prospects, and Challenges. *Adv. Mater.*, 2009, **21**(25–26), P. 2632–2663.
- [7] Chua L. Resistance Switching Memories Are Memristors. *Appl. Phys. A*, 2011, **102**(4), P. 765–783.
- [8] Chua L.O., Kang S.M. Memristive devices and systems. *Proc. IEEE*, 1976, **64**(2), P. 209–223.
- [9] Du C., Ma W., Chang T., Sheridan P., Lu W.D. Biorealistic Implementation of Synaptic Functions with Oxide Memristors through Internal Ionic Dynamics. *Adv. Funct. Mater.*, 2015, **25**(27), P. 4290–4299.
- [10] Pickett M.D., Medeiros-Ribeiro G., Williams R.S. A Scalable Neuristor Built with Mott Memristors. *Nat. Mater.*, 2012, **12**(2), P. 114–117.
- [11] Yang J.Y., Pickett M.D., Li X., Ohlberg D.A.A., Stewart D.R., Williams S. Memristive switching mechanism for metal/oxide/metal nanode- vices. *Nat. Nanotech.* 2008, **3**, P. 429–433.
- [12] Illarionov G.A., Morozova S.M., Chrisotov V.V., Einarsrud M.-A., Morozov M.I. Memristive TiO₂: Synthesis, Technologies, and Applica- tions. *Front. Chem.*, 2020, **8**, P. 724.
- [13] Acharyya D., Hazra A., Bhattacharyya P. A journey towards reliability improvement of TiO₂ based resistive random-access memory: a review. *Microelectron. Reliab.*, 2014, **54**, P. 541–560.
- [14] Xia Q., Robinett W.; W. Cumbie M., Banerjee N., J. Cardinali T., Joshua Yang J., Wu W., Li X., M. Tong W., B. Strukov D., S. Snider G., Medeiros-Ribeiro G., Williams S.R. Memristor?CMOS Hybrid Integrated Circuits for Reconfigurable Logic. *Nano Lett.*, 2009, **9**(10), P. 3640–3645.
- [15] Jeong D.S., Thomas R., Katiyar R.S., Scott J.F. Overview on the Resistive Switching in TiO₂ Solid Electrolyte. *Integr. Ferroelectr.*, 2011, **124**(1), P. 87–96.
- [16] Zhang F., Gan X., Li X., Wu L., Gao X., Zheng R., He Y., Liu X., Yang R. Realization of Rectifying and Resistive Switching Behaviors of TiO₂ Nanorod Arrays for Nonvolatile Memory. *Electrochem. Solid-State Lett.*, 2011, **14**(10), P. H422.
- [17] Xia Q., Yang J.J. Memristive Crossbar Arrays for Brain-Inspired Computing. *Nat. Mater.*, 2019, **18**(4), P. 309–323.
- [18] Ryu J.-H., Kim S. Artificial Synaptic Characteristics of TiO₂/HfO₂ Memristor with Self-Rectifying Switching for Brain-Inspired Computing. *Chaos, Solitons and Fractals*, 2020, **140**, P. 110236.
- [19] Ismail M., Chand U., Mahata C., Nebhen J., Kim S. Demonstration of Synaptic and Resistive Switching Characteristics in W/TiO₂/HfO₂/TaN Memristor Crossbar Array for Bioinspired Neuromorphic Computing. *J. Mater. Sci. Technol.*, 2022, **96**, P. 94–102.
- [20] Fu T., Liu X., Gao H., Ward J.E., Liu X., Yin B., Wang Z., Zhuo Y., Walker D.J.F., Joshua Yang J., Chen J., Lovley D.R., Yao J. Bioinspired Bio-Voltage Memristors. *Nat. Commun.*, 2020, **11**(1), P. 1861.
- [21] Roncador A., Jimenez-Garduco A.M., Pasquardini L., Giusti G., Cornella N., Lunelli L., Potrich C., Bartali R., Aversa L., Verucchi R., Serra M.D., Caponi S., Iannotta S., Macchi P., Musio C. Primary Cortical Neurons on PMCS TiO₂ Films towards Bio-Hybrid Memristive Device: A Morpho-Functional Study. *Biophys. Chem.*, 2017, **229**, P. 115–122.
- [22] Gupta I., Serb A., Khiat A., Zeitler R., Vassanelli S., Prodromakis T. Real-Time Encoding and Compression of Neuronal Spikes by Metal- Oxide Memristors. *Nat. Commun.*, 2016, **7**, P. 12805.
- [23] Serb A., Corna A., George R., Khiat A., Rocchi F., Reato M., Maschietto M., Mayr C., Indiveri G., Vassanelli S., Prodromakis T. Memristive Synapses Connect Brain and Silicon Spiking Neurons. *Sci. Rep.*, 2020, **10**(1).
- [24] Vidiš M., Plecenik T., Movško M., Tomavšec S., Roch T., Satrapinskyy L., Gran?i? B., Plecenik A. Gasistor: A Memristor Based Gas- Triggered Switch and Gas Sensor with Memory. *Appl. Phys. Lett.*, 2019, **115**(9), P. 93504.
- [25] Sahu D.P., Jammalamadaka S.N. Detection of Bovine Serum Albumin Using Hybrid TiO₂ + Graphene Oxide Based Bio – Resistive Random Access Memory Device. *Sci. Rep.*, 2019, **9**(1), P. 16141.
- [26] Haidry A.A., Ebach-Stahl A., Saruhan B. Effect of Pt/TiO₂ Interface on Room Temperature Hydrogen Sensing Performance of Memristor Type Pt/TiO₂/Pt Structure. *Sensors Actuators B Chem.*, 2017, **253**, P. 1043–1054.

- [27] Vilmi P., Nelo M., Voutilainen J.-V., Palosaari J., Pörhönen J., Tuukkanen S., Jantunen H., Juuti J., Fabritius T. Fully Printed Memristors for a Self-Sustainable Recorder of Mechanical Energy. *Flex. Print. Electron.*, 2016, **1**(2), P. 25002.
- [28] Senthilkumar V., Kathalingam A., Kannan V., Rhee J.-K. Observation of Multi-Conductance State in Solution Processed Al/a-TiO₂/ITO Memory Device. *Microelectron. Eng.*, 2012, **98**, P. 97–101.
- [29] Yoshida C., Tsunoda K., Noshiro H., Sugiyama Y. High Speed Resistive Switching in Pt/TiO₂/TiN Film for Nonvolatile Memory Application. *Appl. Phys. Lett.*, 2007, **91** (22), P. 223510.
- [30] Park J., Jung S., Lee J., Lee W., Kim S., Shin J., Hwang H. Resistive Switching Characteristics of Ultra-Thin TiOx. *Microelectron. Eng.* 2011, **88**(7), P. 1136–1139.
- [31] Do Y.H., Kwak J.S., Hong J.P., Jung K., Im H. Al Electrode Dependent Transition to Bipolar Resistive Switching Characteristics in Pure TiO₂ Films. *J. Appl. Phys.*, 2008, **104**(11), P. 114512.
- [32] Wei Z., Kanzawa Y., Arita K., Katoh Y., Kawai K., Muraoka S., Mitani S., Fujii S., Katayama K., Iijima M., Mikawa T., Ninomiya T., Miyayama R., Kawashima Y., Tsuji K., Himeno A., Okada T., Azuma R., Shimakawa K., Sugaya H., Takagi T., Yasuhara R., Horiba K., Kumigashira H., Oshima M. Highly Reliable TaOx ReRAM and Direct Evidence of Redox Reaction Mechanism. In 2008 IEEE International Electron Devices Meeting; 2008, P. 1–4.
- [33] Yang J.J., Zhang M.-X., Strachan J.P., Miao F., Pickett M.D., Kelley R.D., Medeiros-Ribeiro G., Williams R.S. High Switching Endurance in TaOx Memristive Devices. *Appl. Phys. Lett.*, 2010, **97**(23), P. 232102.
- [34] Tao D.W., Chen J.B., Jiang Z.J., Qi B.J., Zhang K., Wang C.W. Making reversible transformation from electronic to ionic resistive switching possible by applied electric field in an asymmetrical Al/TiO₂/FTO nanostructure. *Appl. Surf. Sci.*, 2020, **502**, P. 144124.
- [35] Hu L., Han W., Wang H. Resistive switching and synaptic learning performance of a TiO₂ thin film based device prepared by sol-gel and spin coating techniques. *Nanotechnology*, 2020, **31**, P. 155202.
- [36] Dai Y., Bao W., Hu L., Liu C., Yan X., Chen L., et al. Forming free and ultralow-power erase operation in atomically crystal TiO₂ resistive switching. *2D Materials*, 2020, **4**, P. 025012.
- [37] Xiao M., Musselman K.P., Duley W.W., Zhou N.Y. Resistive switching memory of TiO₂ nanowire networks grown on Ti foil by a single hydrothermal method. *Nano-Micro Lett.*, 2017, **9**, P. 15.
- [38] Dongale T.D., Shinde S.S., Kamat R.K., Rajpure K.Y. Nanostructured TiO₂ thin film memristor using hydrothermal process. *J. Alloy. Compounds.*, 2014, **593**, P. 267–270.
- [39] Abunahla H., Mohammad B., Mahmoud L., Darweesh M., Alhawari M., Jaoude M.A., et al. Memsens: memristor-based radiation sensor. *IEEE Sens. J.*, 2018, **18**, P. 3198–3205.
- [40] Illarionov G.A., Kolchanov D.S., Mukhin I.S., Kuchur O.A., Zhukov M.V., Sergeeva E., et al. Inkjet assisted fabrication of planar biocompatible memristors. *RSC Adv.*, 2019, **9**, P. 35998–36004.
- [41] Vilmi P., Nelo M., Voutilainen J.V., Palosaari J., Pörhönen J., Tuukkanen S., et al. Fully printed memristors for a self-sustainable recorder of mechanical energy. *Flex. Print. Electron.*, 2016, **1**, P. 025002.
- [42] Szot K., Speier W., Bihlmayer G., Waser R. Switching the electrical resistance of individual dislocations in single-crystalline SrTiO₃. *Nature Mater.*, 2006, **5**(4), P. 312–320.
- [43] Yang J., Miao F., Pickett M.D., Ohlberg D.A.A., Stewart D.R., Lau C.N., Williams R.S. The mechanism of electroforming of metal oxide memristive switches. *Nanotechnology*, 2009, **20**(21), P. 215201.
- [44] Jang M.H., Agarwal R., Nukala P., Choi D., Johnson A.T.C., Chen I.-W., Agarwal R. Observing Oxygen Vacancy Driven Electroforming in Pt-TiO₂-Pt Device via Strong Metal Support Interaction. *Nano Lett.*, 2016, **16**(4), P. 2139–2144.
- [45] Münstermann R., Yang J.J., Strachan J.P., Medeiros-Ribeiro G., Dittmann R., Waser R. Morphological and electrical changes in TiO₂ memristive devices induced by electroforming and switching. *Physica Status Solidi (RRL) - Rapid Research Letters*, 2010, **4**(1-2), P. 16–18.
- [46] Prusakova V., Dire S., Collini C., Pasquardini L., Vanzetti L., Resta G., Pederzoli C., Lorenzelli L. Optimisation and Memristive Response of Sol-Gel Derived TiO₂ thin films. In Proc. XVIII AISEM Annual Conference. AISEM 2015, IEEE Inc. 2015.
- [47] Schroeder H., Jeong D.S. Resistive switching in a Pt/TiO₂/Pt thin film stack – a candidate for a non-volatile ReRAM. *Microelectronic Engineering*, 2007, **84**(9-10), P. 1982–1985.
- [48] Waser R., Aono M. Nanoionics-Based Resistive Switching Memories. *Nanosci. Technol. A Collect. Rev. from Nat. Journals*, 2009, P. 158–165.
- [49] Kwon D.-H., Lee S., Kang C.S., Choi Y.S., Kang S.J., Cho H.L., Sohn W., Jo J., Lee S.-Y., Oh K.H., Noh T.W., De Souza R.A., Martin M., Kim M. Unraveling the Origin and Mechanism of Nanofilament Formation in Polycrystalline SrTiO₃ Resistive Switching Memories. *Adv. Mater.*, 2019, **31**(28), P. 1901322.
- [50] Kim K.M., Choi B.J., Koo B.W., Choi S., Jeong D.S., Hwang C.S. Resistive Switching in Pt/Al₂O₃/TiO₂/Ru Stacked Structures. *Electrochem. Solid-State Lett.*, 2006, **9**(12), P. G343.
- [51] Schroeder H., Jeong D.S. Resistive switching in a Pt/TiO₂/Pt thin film stack – a candidate for a non-volatile ReRAM. *Microelectron. Eng.*, 2007, **84**, P. 1982.
- [52] Münstermann R., Yang J.J., Strachan J.P., Medeiros-Ribeiro G., Dittmann R. and Waser R. Morphological and electrical changes in TiO₂ memristive devices induced by electroforming and switching. *phys. stat. sol. (RRL)*, 2010, **4**, P. 16–18.
- [53] Yuzhakov V., Chang H.-C., Miller A. Pattern Formation during Electropolishing. *Phys. Rev. B*, 1997, **56**, P. 12608–12624.
- [54] Yuzhakov V.V., Takhistov P.V., Miller A.E., Chang H.-C. Pattern Selection during Electropolishing Due to Double-Layer Effects. *Chaos Interdiscip. J. Nonlinear Sci.*, 1999, **9**(1), P. 62–77.